

Electronic Supplementary Material (ESI) for ChemComm

Organotin(IV) Differential Fluorescent Probe for Controlled-Subcellular Localization and Nuclear Microviscosity Monitoring

*Jasmine Bernal-Escalante, † Armando López-Vázquez, † Daniela Araiza-Olivera, and Arturo Jiménez-Sánchez †,**

† Instituto de Química, Universidad Nacional Autónoma de México, México D.F. No. 04510, México.

AUTHOR INFORMATION

Corresponding author arturo.jimenez@iquimica.unam.mx

Department of Organic Chemistry
Institute of Chemistry - Universidad Nacional Autónoma de México.
Circuito Exterior, Ciudad Universitaria, Ciudad de México, Mexico.
E-mail: arturo.jimenez@iquimica.unam.mx

** **Financial support by PAPIIT-UNAM IA201318 is greatly acknowledged. We also acknowledge the assistance of M. en C. Lucero Mayra Rios Ruiz and M. En C. Lucía del Carmen Márquez for HPLC. We acknowledge assistance of Miguel Tapia Rodríguez (Ph.D. IIBO, UNAM) and Abraham Rosas Arellano (PhD. Unidad de Imagenología del IFC-UNAM) in imaging microscopy and Salvador Ramírez Jiménez (Biol. IIBO, UNAM) in tissue culture, Laboratorio Nacional de Ciencias para la Conservación del Patrimonio Cultural (LANCIC, Projects: LN 232619, LN 260779, LN 279740 and LN 271614, Instituto de Química) by CONACyT and Everardo Tapia Mendoza (MS), Beatriz Quiroz García (NMR) from the LURMN at IQ-UNAM, which is founded by CONACyT Mexico (Project: 0224747) and UNAM.**

| Experimental procedure | Page |
|--|-------------|
| Materials and methods | 2 |
| General probe synthesis, purification and chemical characterization, Scheme S1 | 2 – 7 |
| Figures S1 | 8 |
| Figure S2 | 9 |
| Figure S3 | 10 |
| Table S1 | 11 |
| Figure S4 | 12 |
| Scheme S2 | 13 |
| Figure S5 | 14 |
| Table S2 and Figure S6 | 15 |
| Figure S7-S8 | 16 |
| Figure S9 | 17-18 |
| Table S3 | 19 |
| References | 20 |

Experimental Procedures

Materials and Methods

Cell Culture

SK-LU-1 and HeLa cells were cultured in Minimum Essential Medium Alpha (MEM alpha, Gibco, Gaithersburg MD) supplemented with 10% fetal bovine serum (FBS, Invitrogen, Carlsbad CA) at 37°C with 5% CO₂.

Live Cell Measurements

Live SK-LU-1 and HeLa cells were seeded in three different 8-well μ -slides at a density of 10 000 cells per well for 12 hours prior experiments using RPMI medium supplemented with 10 FBS. Then, specific concentrations of **HQN**, nBu₂(Sn)Cl₂, adenosine monophosphate (AMP), and specific metal ions and polyols in RPMI media were added on each slide 30 minutes before imaging experiments. For nuclear and cytoplasmic imaging, cell cultures were washed two times with RPMI. During confocal imaging the microscope parameters were maintained constant using a 63x oil immersion objective.

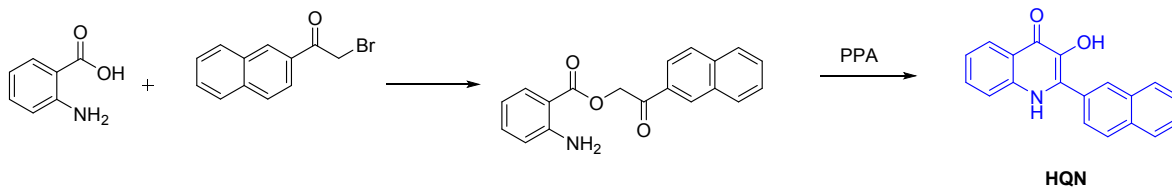
Spectrophotometric and Fluorometric Titrations.

All titration experiments were performed at 25 °C and ionic strength 0.05 M created either by bu \square er or NaCl. The experiments were performed with and without 5 mM hexadecyltrimethylammonium bromide (HTAB). An aliquot of 1 mM stock solution of **HQN** in acetonitrile was added to a 5 mM MOPS aqueous buffered solution in appropriate pH intervals, allowing to equilibrate for 15 minutes before titrations. The final content of acetonitrile remained less 1%. Fluorescence quantum yields of **HQN** and the equimolar nBu₂Sn(**HQN**) complex were 0.17 and 0.08, respectively, obtained according to the relative protocol [S. Fery-Forgues, D. Lavabre, *J. Chem. Educ.*, 1999, **76**, 1260.] using coumarin 6 in ethanol as standard fluorophore.

Quantum Chemical Calculations

Quantum Chemical Calculations were obtained by using DFT and TD-DFT with Polarizable Continuum Model¹ as performed in the Gaussian 09 code,² using a PBE0/6-31+G(d,p)/IEF-PCM (water) level of theory to determine the optimized molecular geometry of **HQN**. Then, a frequency analysis corroborates that the geometry corresponds to an energy minimum, finding no imaginary frequencies. As a first step in the analysis of the electron charge distribution in the molecules, the electrostatic potentials were computed to compare the local charge distribution between these molecules. Finally, Natural Transition Orbital (NTO)³ analysis was computed at the same level of theory to further understand the optical properties for probe **HQN**.

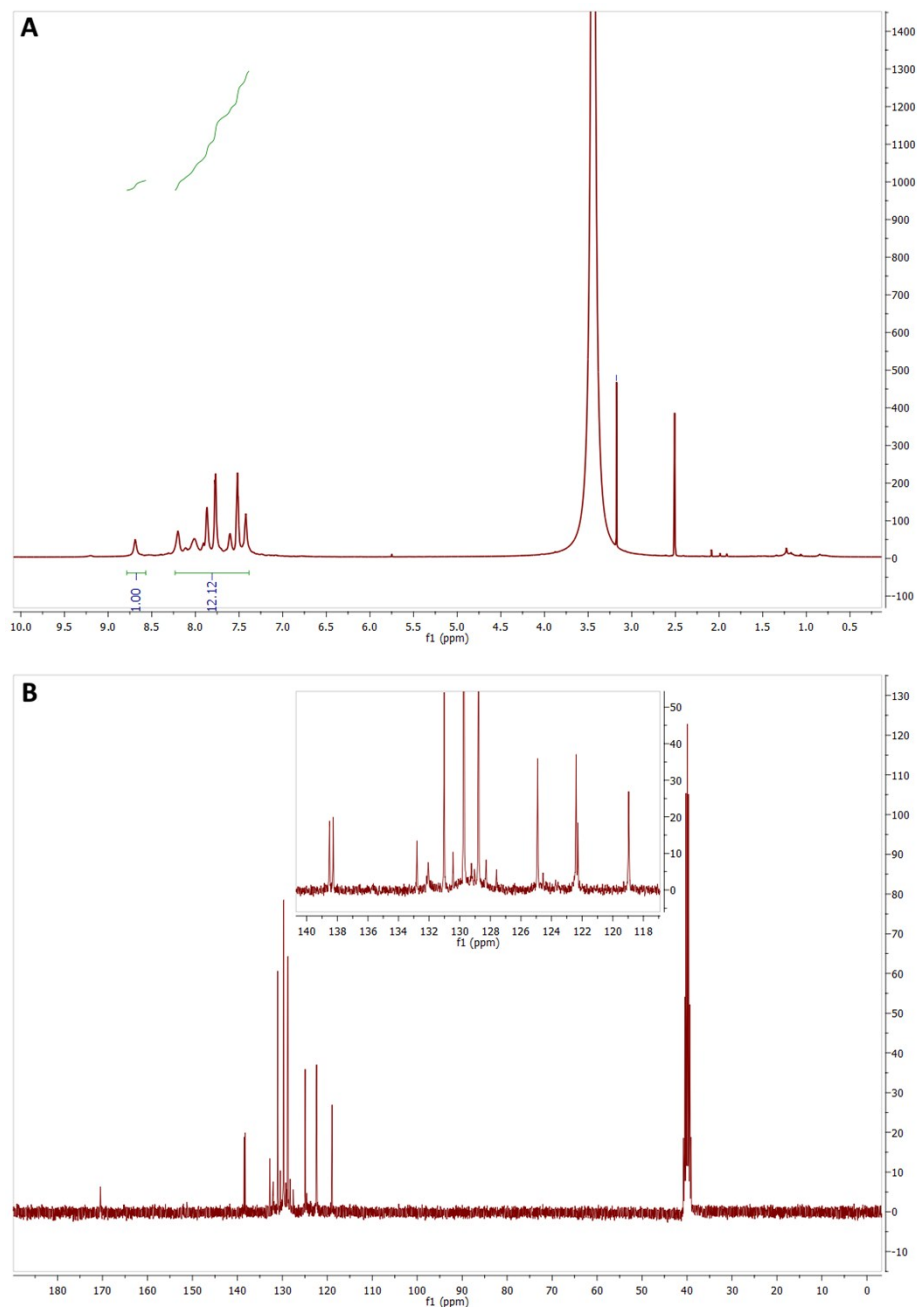
General Probe Synthesis



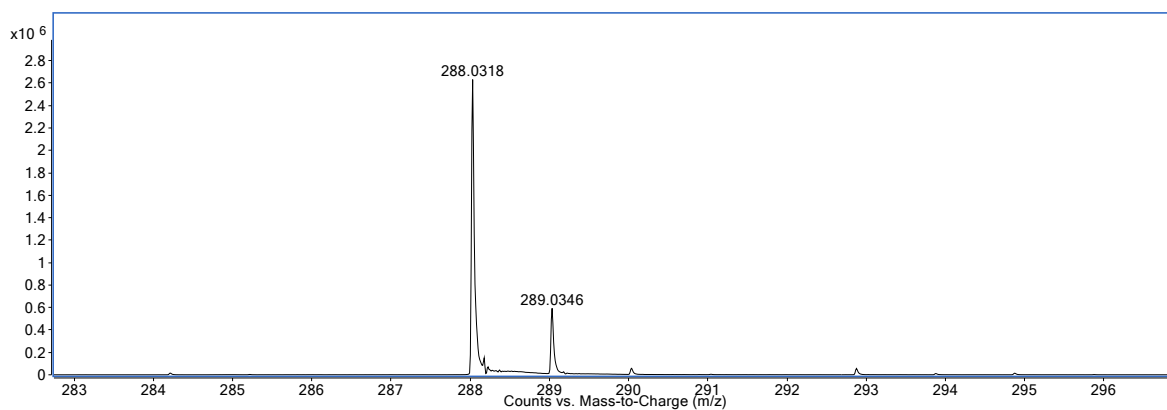
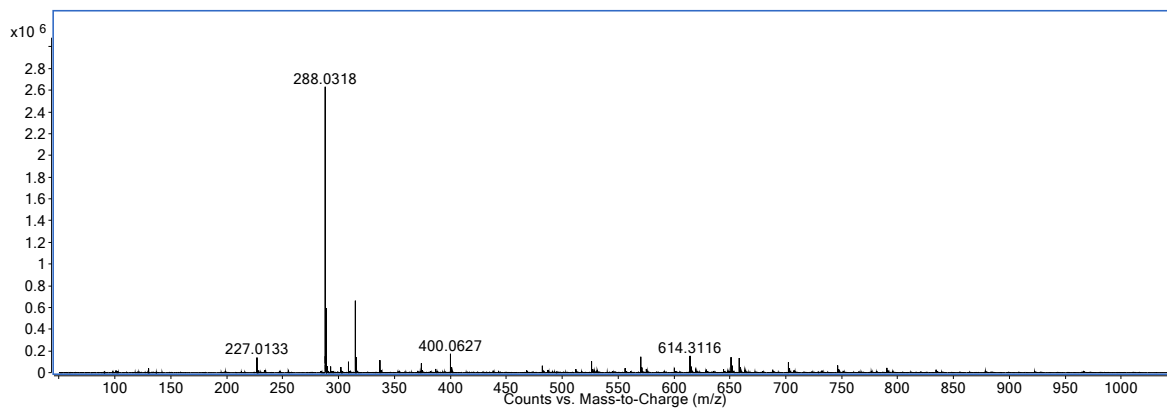
Scheme S1. Synthetic methodology for probe **HQN**.

*Synthetic procedure for 2-naphthyl-3-hydroxy-4(1H)-quinolone (**HQN**).* Compound **HQN** was synthesized as described in literature for other similar structures [P. Hradil, J. Hlaváč, K. Lemr, *J. Heterocyclic Chem.*, 1999, **36**, 141–144.]. A solution of 3-Aminobenzoic acid (2.00 g, 14.50 mmol) dissolved in DMF (20 mL) was mixed with potassium carbonate anhydrous (2.16 g, 15.6 mmol). Then, the reaction mixture was heated to 90 °C and stirred for 1 h. After that, the solution was cooled to 20 °C and 2-Bromo-2'-naphthylacetone (2.00 g, 8.02 mmol) was added. The generated exothermic reaction was stirred for 30 min, at this temperature. Then, the reaction was heated to 60 °C and stirred

for 30 min more. The product was poured in cooled water and the precipitated product was collected by filtration, washed with water (3 x 30 mL) and dried. After that, the anthranilate (0.5 g, 1.48 mmol) was added to a previously heated polyphosphoric acid (5.0 g) and stirred at 120 °C during 2 h. The reaction mixture was poured into cooled water (10 g), then the pH was adjusted to 7 – 8 with a NaOH 10% solution and the precipitated solid was collected by filtration, washed with water (3 x 30 mL), dried and recrystallized from DMF. ¹H NMR (300 MHz; DMSO-d₆; Me₄Si): δ 9.21 (br. s, 1H), 8.19-7.42 (m, 12H), ¹³C NMR (300 MHz; DMSO-d₆; Me₄Si): δ 171.0, 138.5, 138.2, 132.8, 132.2, 132.0, 131.0, 130.4, 129.7, 129.2, 128.3, 128.2, 127.6, 127.5, 124.9, 124.6, 122.4, 122.3, 118.9. IR (ν_{max}/cm⁻¹) 3440 (O–H stretching), 2994, 2913, 2845 (C–H stretching), 1663 (C=O stretching). MS (ESI, m/z) for C₁₉H₁₃N₁O₂: [M]⁺ calculated: 287.03, found [M+H]⁺: 288.0918, error = 0.012 ppm m.p. 262–264 °C.



(A) ¹H and (B) ¹³C NMR spectra of probe HQN in DMSO-δ₆.



HRMS ESI[+] spectrum of probe **HQN** for $C_{19}H_{13}N_1O_2 = M$; $[M+H]^+$: 288.0318

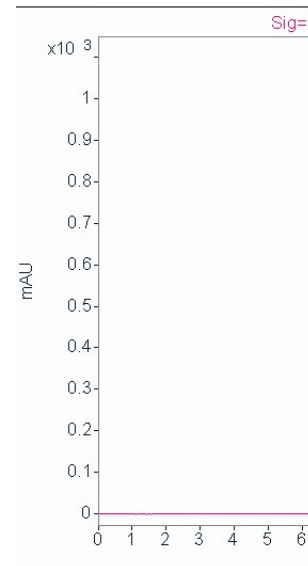
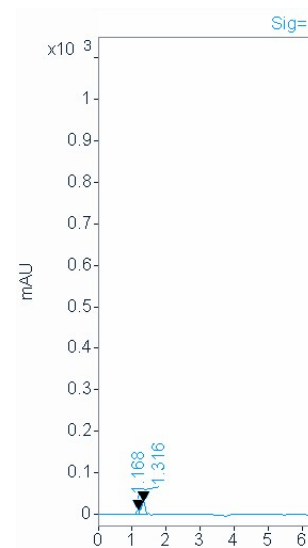
HPLC Purification

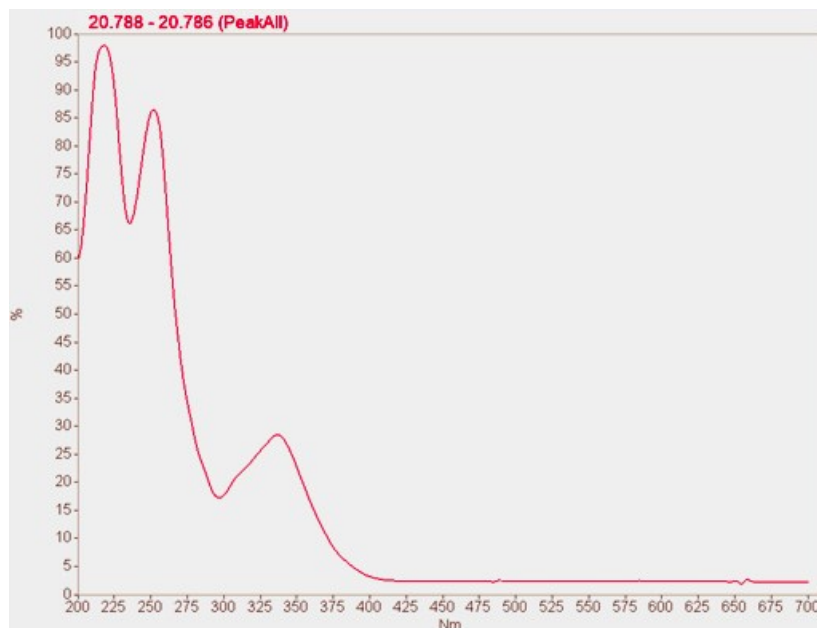
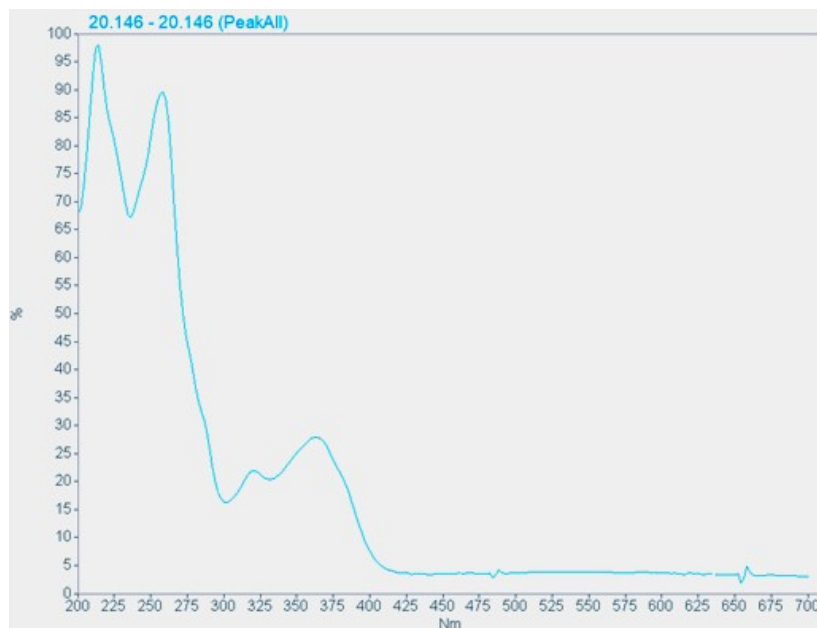
A 50 μ M stock solution of Compound **5** in PBS was run through RP-HPLC on a C18 column with a 10-70% MeCN/H₂O 2%/min gradient with 0.1% TFA. Retention time is shown below. The peaks were identified through a UV-Vis detector at different wavelengths (below is shown 360 nm before and after purification).

Sample:
HQN

| | | | |
|-------------------|---|-------|----|
| HPLC | Agilent 1260 Infinity II | | |
| Detector | UV-Vis | | |
| Wavelength | 360 nm | | |
| Column | Kinetex XB C18 50 x 2.1 mm 2.6 μm | | |
| Eluent | acetonitrile | Water | |
| | Inicial | 10 | 90 |
| | 30 min | 70 | 30 |
| Flux | 0.2 mL/min | | |

Date 26-01-2019





UV-Vis traces for the HQN before (blue) and after purification (red).

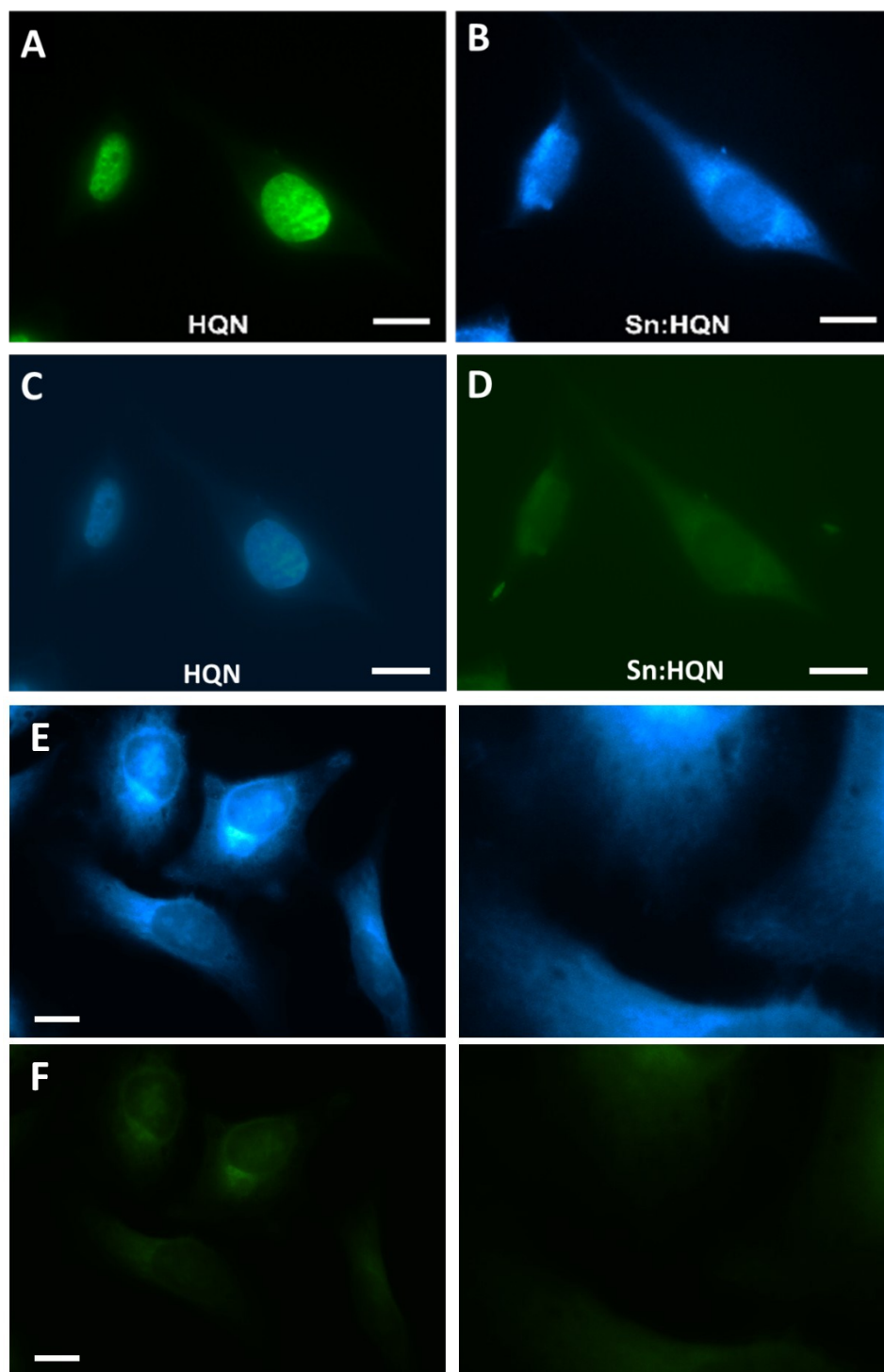


Figure S1. Intracellular localization redistribution of the **HQN** in live SK-LU-1 cells under 30 minutes incubation observed in (A) the confocal green channel ($\lambda_{\text{exc}} = 503 \text{ nm}$, $\lambda_{\text{em}} = 550 \text{ nm}$) and in (C) the blue channel ($\lambda_{\text{exc}} = 404 \text{ nm}$, $\lambda_{\text{em}} = 470 \text{ nm}$), indicating a strong nuclear localization. Then, the $\text{Sn}(n\text{Bu})_2\text{Cl}_2$ addition (45 minutes incubation) enable a clean cytosol distribution observed in (B) the blue channel ($\lambda_{\text{exc}} = 404 \text{ nm}$, $\lambda_{\text{em}} = 470 \text{ nm}$) and in (D) the green channel ($\lambda_{\text{exc}} = 503 \text{ nm}$, $\lambda_{\text{em}} = 550 \text{ nm}$). Control experiments showing the localization using the equimolar performed Sn:HQN complex observed under the blue (E) and green (F) channels. Scale bars represent $20 \mu\text{m}$.

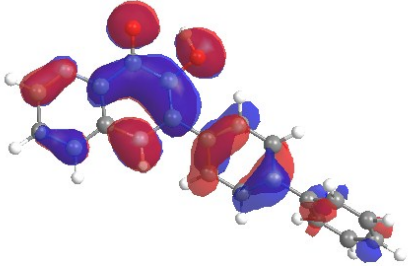
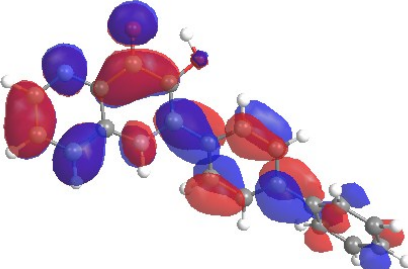
| | NTO – Hole | NTO – Particle |
|--|---|--|
| NTO eigenvalue $w = 0.98$ $f = 0.289$ 3.314 eV For the HOMO – LUMO levels |  |  |

Figure S2. The dominant natural transition orbital pair for the first excited singlet state of **HQN**. The left panels quote in sequence the NTO eigenvalue (w), oscillator strength (f), transition energy, and associated MO levels.

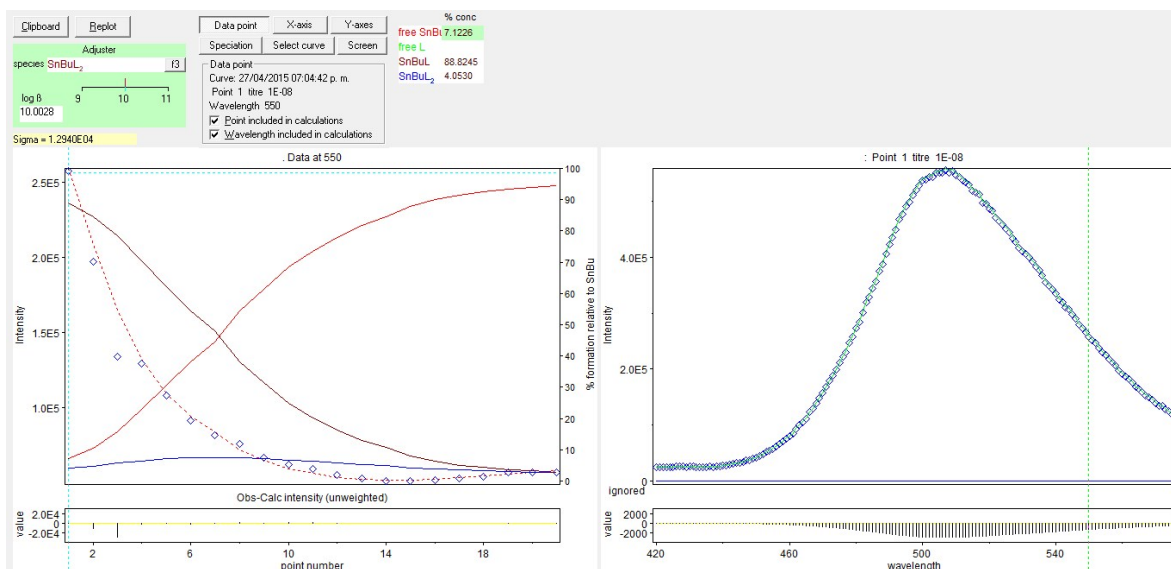
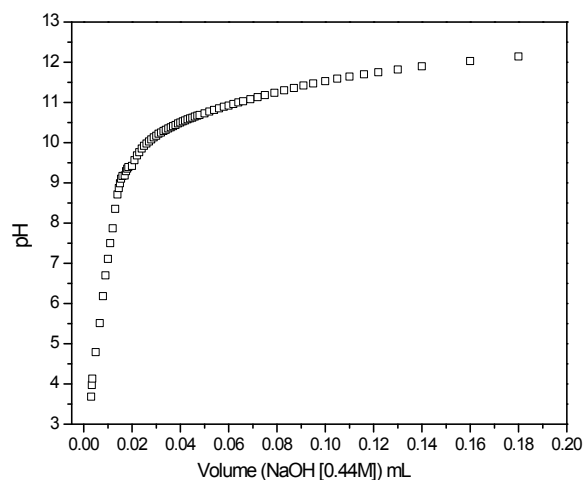
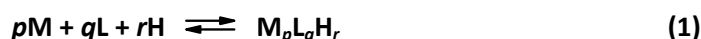


Figure S3. Potentiometric titration in 10 mL **HQN** thermostatted at 25 °C under N₂ using 0.05 M NaCl as background electrolyte to maintain ionic strength, pH was 7 under 5 mM HTAB media. Below: the potentiometric data analyzed with HyperQuad software when detecting at 550 nm. L stands for the **HQN** ligand while SnBu for Sn(*n*Bu)₂Cl₂. As can be seen from the iteration data and the Figure below, about 89% of the equimolar [*n*Bu₂Sn]**HQN** complex is strongly favored over competing [*n*Bu₂Sn]**HQN**₂ stoichiometry and the free ligand, indicating that this complex is dominant under such conditions.

Table S1. Protonation constants of ligands and stability constants of metal complex determined potentiometrically in 20% vol. acetonitrile, 0.05 M NaCl at 25°C.

| species | p q r | log β_{pqr} | equilibrium | log K_{obs} |
|--------------------------------|-------|-------------------|--|---------------|
| LH | 0 1 1 | 11.08±0.01 | L + H = LH | 11.90 |
| LH ₂ | 0 1 2 | 20.42±0.01 | LH + H = LH ₂ | 10.66 |
| <i>n</i> Bu ₂ Sn LH | 1 1 1 | 24.17±0.09 | <i>n</i> Bu ₂ Sn + LH = <i>n</i> Bu ₂ Sn(LH) | 13.09 |

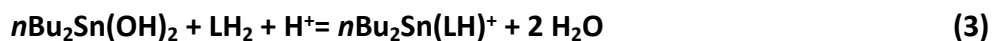
The results of potentiometric titrations were analyzed in terms of traditional *pqr* scheme expressed by equations (1) and (2), where L is a completely deprotonated dianionic form of the HQN ligand and M is the metal ion (*n*Bu₂Sn²⁺). The overall binding constants and the p*K*_a values of free HQN and the complex are collected in Table S2.



$$\beta_{pqr} = [M_pL_qH_r]/[M]^p[L]^q[H]^r \quad (2)$$

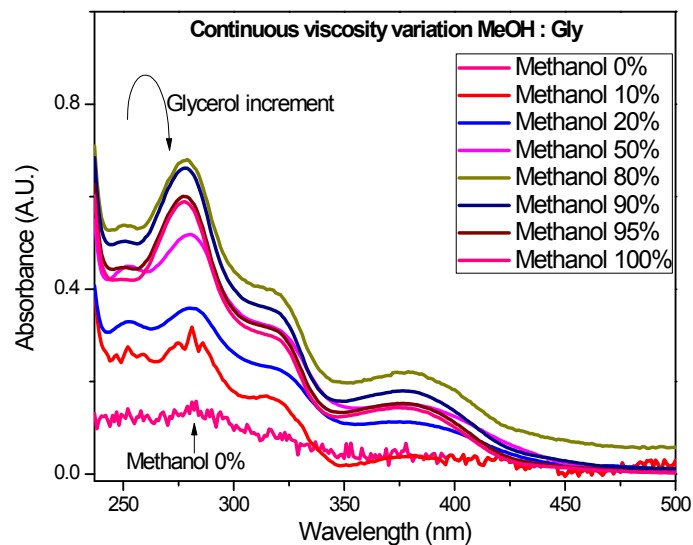
The simple 1 : 1 *n*Bu₂Sn²⁺ complex of the type M(LH)⁺ is much more stable and is a dominating species in acid and neutral solutions. However, with excess of the ligand and pH above 7 the M(LH)₂ complex will be favored.

The stability constant for *n*Bu₂Sn(HL)⁺ complex is in fact larger than expected for other metal ions present in biological systems (Zn²⁺, Cu²⁺, etc).⁴ The reason for this effect is the strong hydrolysis of *n*Bu₂Sn²⁺ cation in neutral solutions. In accordance with reported hydrolysis constants of *n*Bu₂Sn²⁺ in water at pH 7 (log β_{10-2} = -8.30)⁵ the cation is completely transformed into dihydroxo complex and the actual reactions of the formation of M(HL)⁺ is (3).



The corresponding values for K_{obs} at pH = 7 are log K_{obs} = log β_{111} – log β_{012} – log β_{10-2} – pH = (24.17) – (20.42) – (-8.30) – 7.0 = 5.05 for *n*Bu₂Sn(LH)⁺.

(A)



(B)

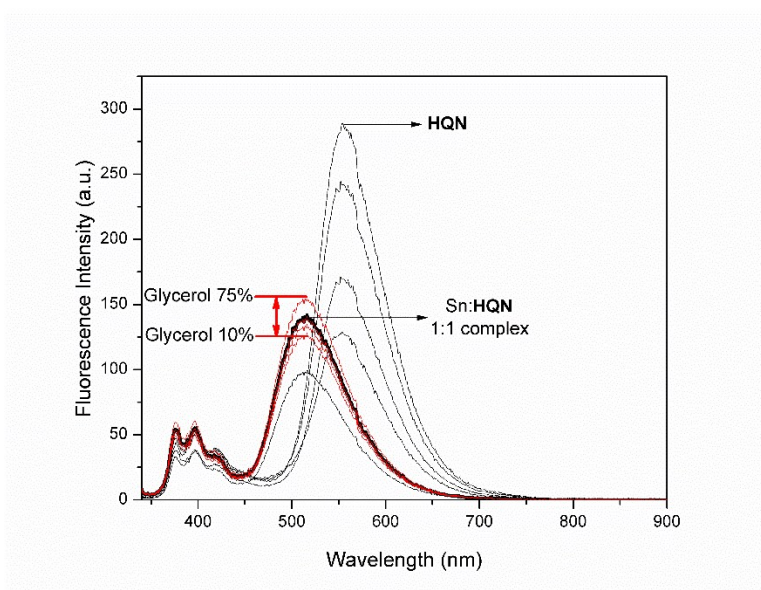
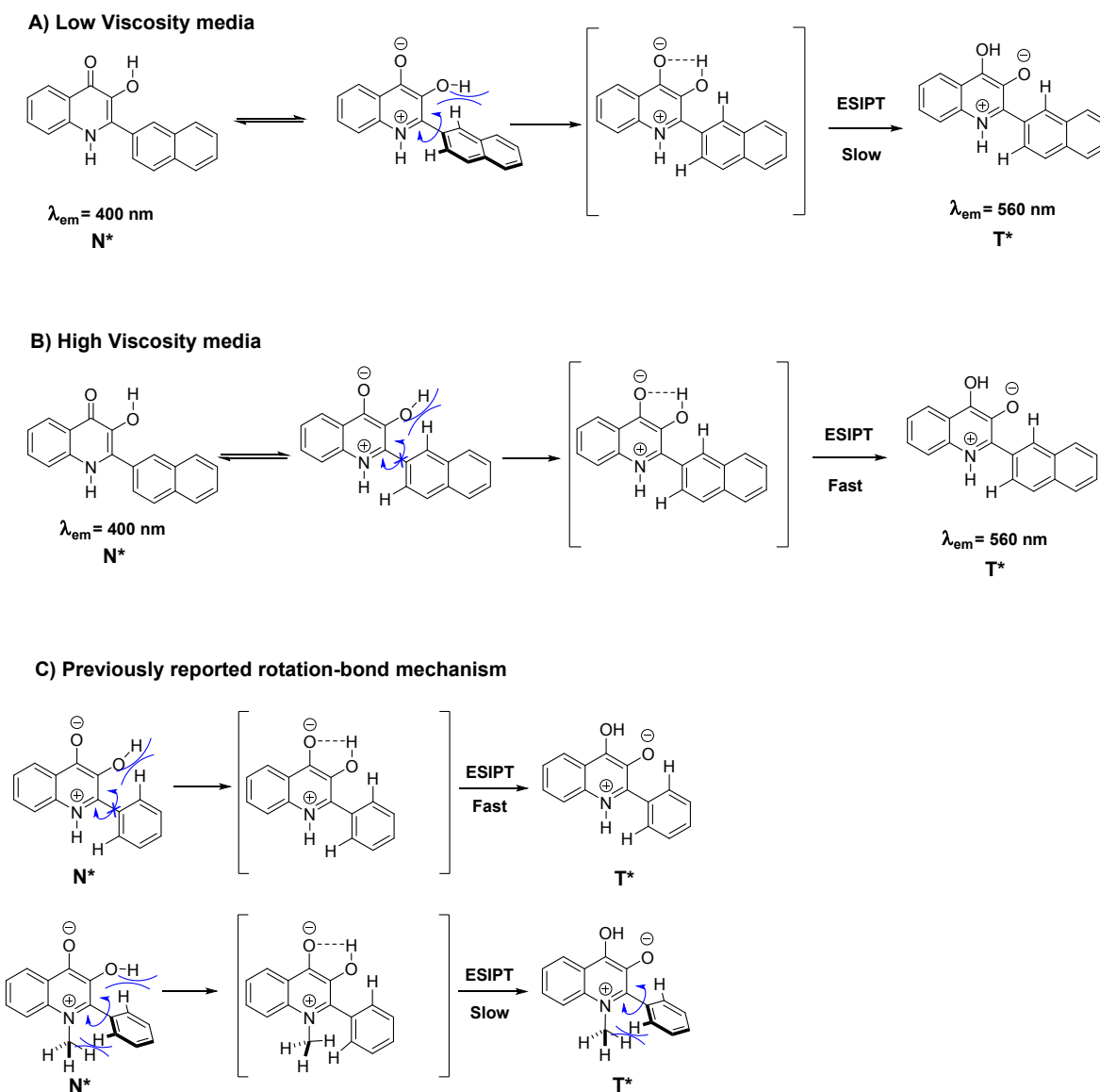


Figure S4. (A) Absorption spectra of 40 μ M HQN at variable viscosity increments. (B) Fluorescence spectra of Sn:HQN (1:1) complex under a continuous viscosity variation from 10% aqueous glycerol to 75% aqueous glycerol.



Scheme S2. Interaction between the 3-hydroxy group and the 2-naphthyl moiety. In (a) a low viscosity media the larger rotational freedom of the naphthyl group decreases the planarity of the dye, enabling a fast ES IPT process, whereas the high viscosity media (b) limits considerably the rotational motion of the naphthyl group giving rise to a slow ES IPT process (T^* tautomer is favored). (c) Previously reported rotation-bond mechanism (*J. Phys. Chem. A*, 2007, **111**, 8986.): Above: Interaction between the 3-hydroxy group and the 2-phenyl moiety in the N-H derivative limits considerably the rotational motion of the hydroxyl group. Below: the steric effect of the proximal N-methyl group decreases the planarity of the dye, enabling a larger rotational freedom of the 3-OH group.

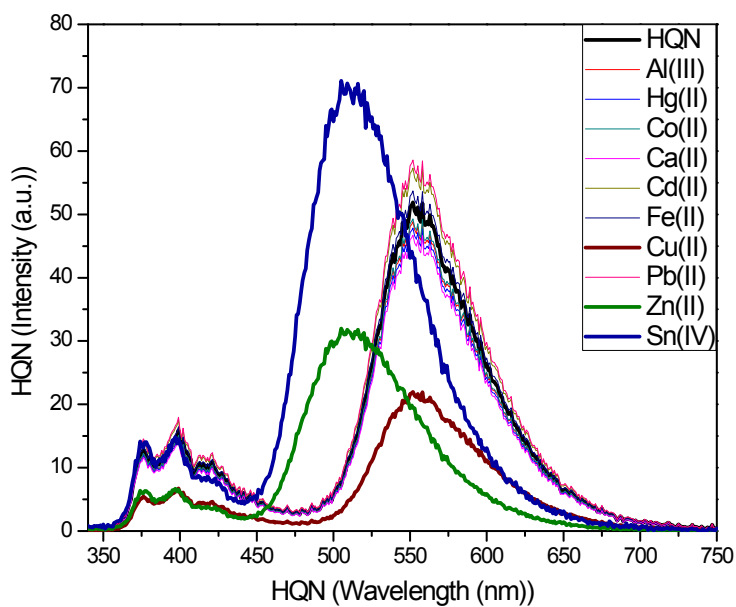
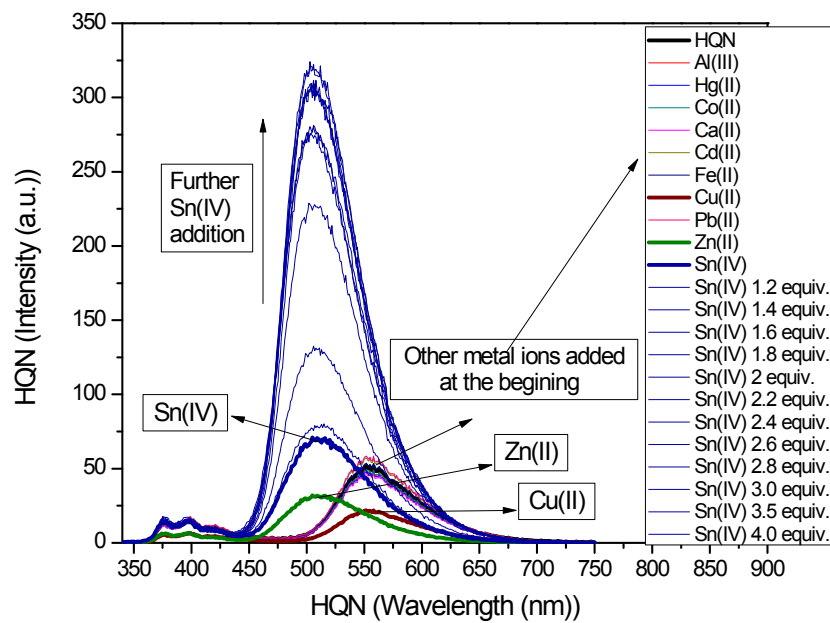


Figure S5. Fluorescence spectra ($\lambda_{\text{exc}} = 330 \text{ nm}$) of $40 \mu\text{M}$ HQN in HTAB 5 mM at variable concentration of different metal ions using stock solutions of $10 \mu\text{M}$, and 50 mM NaCl at $25 \text{ }^\circ\text{C}$.

Table S2. Detailed experimental procedure for *in-vitro* viscosity determinations: The viscosity quantification was done by using the calibration plot obtained in Fig. 1B inset, the Table S1 (below) shows the corresponding viscosity values in cP for each volume fraction of glycerol. Then, the λ -ratiometric method was used by taking the blue signal (at 405 nm) as internal reference since the blue emission channel of the microscope showed no intensity variations during recordings when detecting at the same wavelength $\lambda_{em} = 405$ nm.

| Glycerol volume fraction x_{gly} | Viscosity [cP] |
|------------------------------------|----------------|
| 0.0 | 0.6 |
| 0.1 | 1.8 |
| 0.2 | 4.8 |
| 0.3 | 7.7 |
| 0.4 | 13 |
| 0.5 | 28 |
| 0.6 | 58 |
| 0.7 | 130 |
| 0.8 | 250 |
| 0.9 | 630 |
| 1.0 | 1410 |

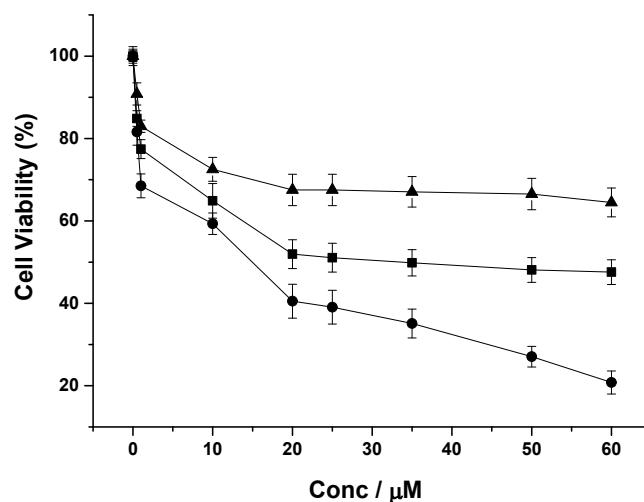


Figure S6. Percentage of SK-LU-1 cell viability remaining after treatment. Cells were grown under standard conditions and treated with: triangles (Sn:HQN), squares (free HQN) and circles ($n\text{Bu}_2\text{SnCl}_2$). Untreated cells were considered to have 100% survival. Cell viability was determined by a redox indicator (Alamar Blue). For cytotoxicity assays, human lung adenocarcinoma (SK-LU-1) cell lines were plated in 96-well plates at 5000 cells/well in RPMI-1640 medium. About 24 h after plating, varied doses of compound Sn:HQN, HQN and $n\text{Bu}_2\text{SnCl}_2$ at 0.5, 1, 10, 20, 25, 35, 50 and 60 μM concentration were added in triplicate. Cell viability was evaluated after 72-h incubation with the molecules using Alamar Blue fluorescent assay (Life Technologies, Carlsbad, CA, USA).

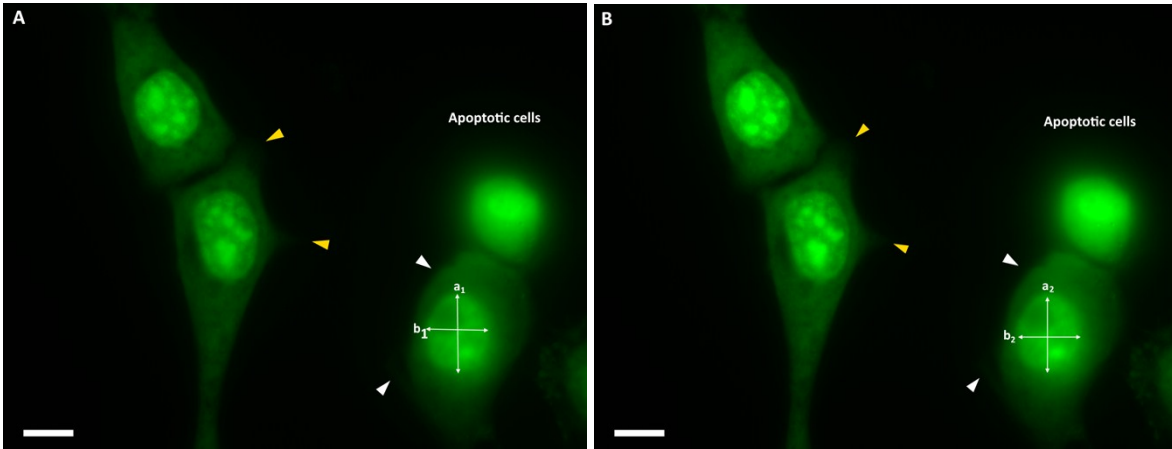


Figure S7. Confocal imaging of the **HQN** in apoptotic HeLa cells treated with high-dose H_2O_2 for 45 min under (A) non-swelling and (B) swelling conditions. Panel (B) shows a 10 minutes time lapse observed in the green channel ($\lambda_{exc} = 503 \text{ nm}$, $\lambda_{em} = 550 \text{ nm}$). Scale bars represent $10 \mu\text{m}$. Distances are $a_1 = 17 \mu\text{m}$ and $b_1 = 13 \mu\text{m}$, while $a_2 = 21 \mu\text{m}$ and $b_2 = 16 \mu\text{m}$. Arrows indicate zones of plasma membrane adhesion (focal points) having almost no variations. However, white arrows (apoptotic cells) show a significant decrease in adhesion. Laser light was fully shielded between recordings to prevent artifacts and photobleaching.

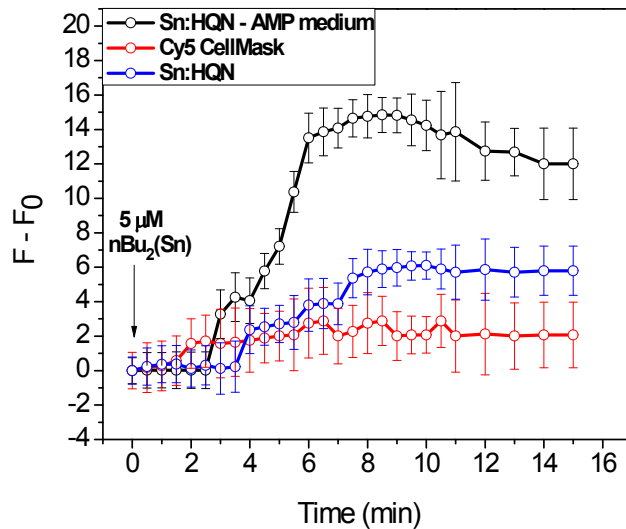
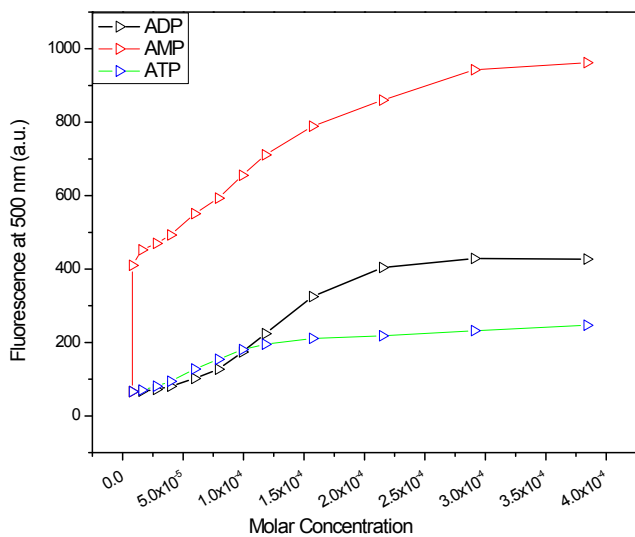
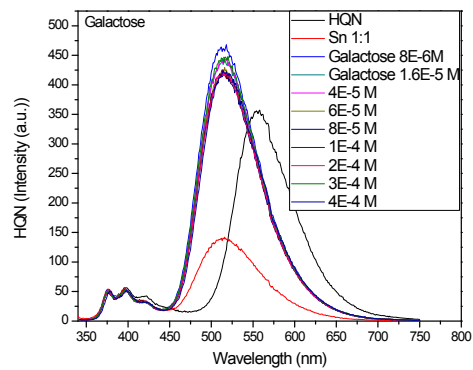
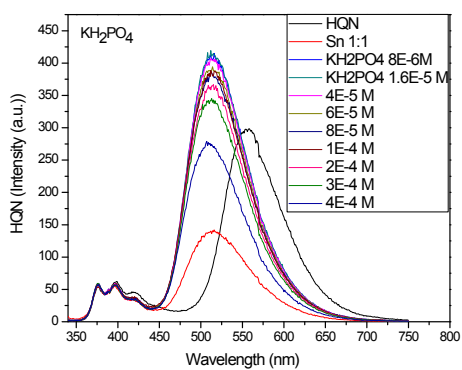
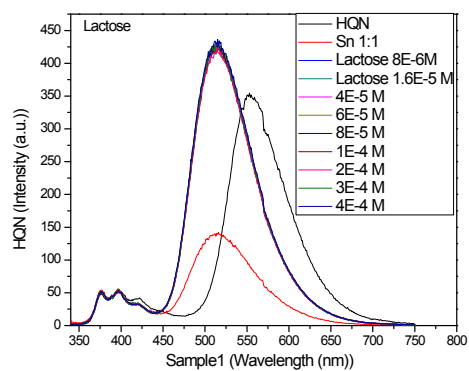
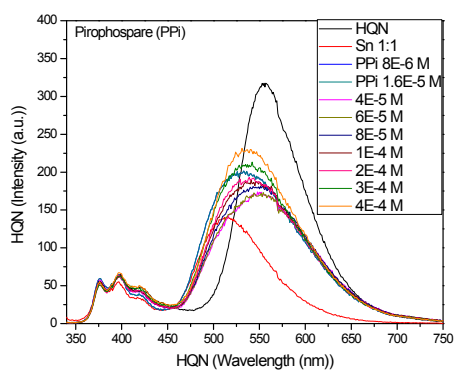


Figure S8. Time-dependent effect of $5 \mu\text{M } n\text{Bu}_2(\text{Sn})$ ion on the **HQN** fluorescence signal, shown as fluorescence difference ($F - F_0$). The experiment was performed in cell culture AMP-enriched MEM medium (dark line) and no AMP-enriched, 2 mg/mL , medium (blue line). Data in red correspond to the fluorescence intensity control **Cy5 CellMask Deep Red** ($\lambda_{ex}/\lambda_{em} = 649/666 \text{ nm}$).

A)



B)



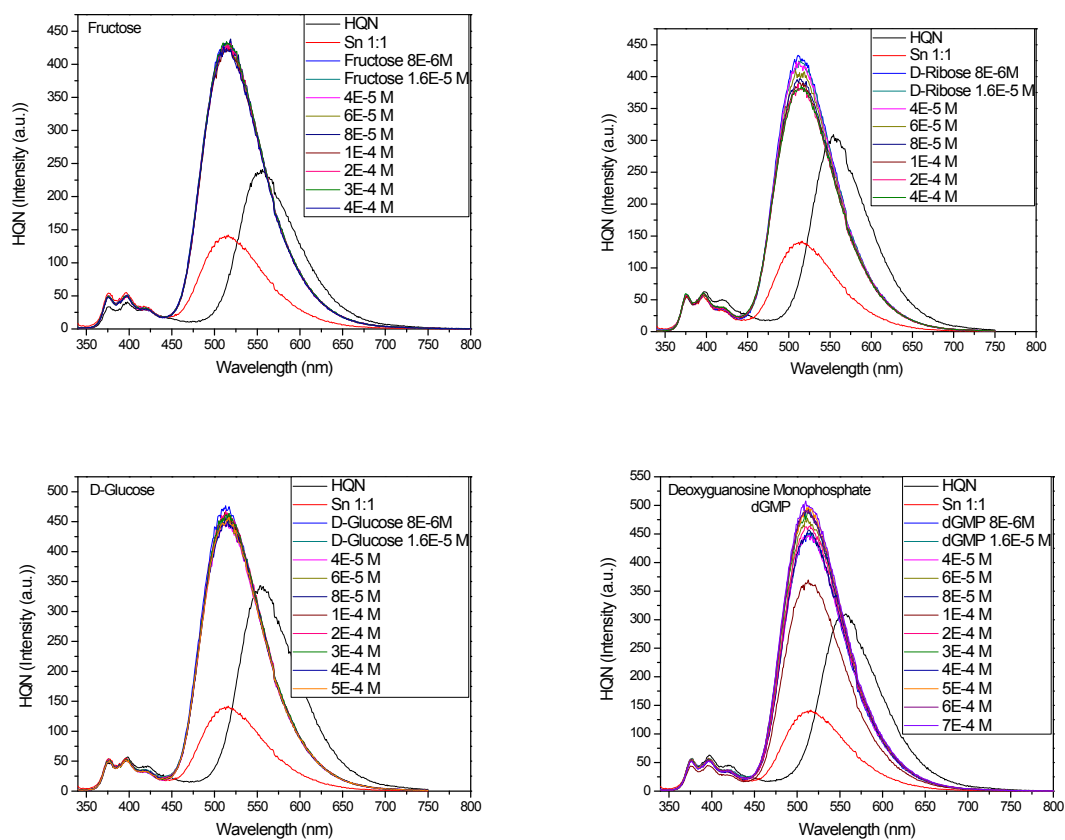


Figure S9. Fluorescent emission titrations ($\lambda_{\text{exc}} = 330 \text{ nm}$) of 10 mM Sn:HQN, under variable concentrations of A) AMP, ADP and ATP anions and; B) a series of polyols. The titrations were conducted at pH = 7.0 in HTAB (5mM) and 10 mM NaCl at 25 °C. Analyte concentrations are shown in the insets.

Table S3. Comparison of different adenosine monophosphate (AMP) detection methods previously reported.

| Reference | Method | Conditions | log K / limit of detection, LoD |
|--|--|--|---|
| Yakun Lian, et.al. <i>Talanta</i> , 2016, 150 , 485. | ^1H and ^{31}P NMR | D ₂ O, peak at 0.9 ppm as quantitative signal of AMP | LoD = 0.40 mM |
| Israel Carreira-Barral, et.al. <i>Molecules</i> , 2018, 23 , 479; doi:10.3390/molecules23020479 | Spectrophotometric | pH = 7, MOPS buffer | log K = 4.35 |
| Li Qin, et.al. <i>Anal. Chem.</i> , 2018, 90 , 9983. | Colorimetric | pH = 7, pretreated sample (digestion) | LoD = 1 μM |
| Sujoy Das, et.al. <i>Chem. Commun.</i> , 2017, 53 , 7600. | Spectrophotometric | pH 7.0, 10 mM HEPES buffer, CH ₃ CN/H ₂ O, 1:6 (v/v) | LoD = 2.8 μM |
| Eisuke Furuya, et.al. <i>Anal. Biochem.</i> , 1985, 145 , 144. | HPLC | Pretreated: glucagon-treated rat liver | LoD = 2 pM |
| Laxman Gangwani, et.al. <i>Biochem. Biophys. Res. Commun.</i> , 1991, 178 , 1113. | HPLC | Pretreated: acidic pH and TLC-purified | LoD = 70-80 pM |
| Mikio Bakke, et.al. <i>J. Food Protect.</i> , 2018, 81 , 729. | Bioluminescence: Total XXXdenylate (ATP+ADP+AMP) | Pretreated: acidic conditions | Not reported Signal rec. 1735 RLU (relative light units) |
| Shan Sun, et.al. <i>Anal. Chem.</i> , 2017, 89 , 5542. | Spectrophotometric | pH = 7.0, Tris buffer, | LoD ~ 1 μM |
| Dhaval P. Bhatt, <i>J. Chromatogr. B</i> , 2012, doi:10.1016/j.jchromb.2012.02.005. | HPLC | Pretreated: pH 4.5 | LoD = 0.16–20.6 pM |
| Subhanjan Mondal, et.al. <i>Assay Drug. Dev. Techn.</i> , 2017, 15 , 330. | Bioluminescence: enzyme-coupled assay | pH 7.5 HEPES buffer | LoD = 100 nM |
| E. Harmsen, et.al. <i>J. Chromatogr.</i> , 1982, 230 , 131. | Ion-exchange chromatography | pH 7.5, UV detector 210 nm | LoD = 20 pM |
| Q. Y. Bai, <i>J. Microbiol. Meth.</i> , 1989, 9 , 345. | Spectrophotometric | pH 7.5 | LoD = 0.05 μM |
| This work | Spectrophotometric | pH ~ 7.4 (cyosol) | log K _{obs} = 4.51±0.01 LoD = 0.038 mM |

References

- [1] a) C. Amovilli, V. Barone, R. Cammi, E. Cancès, M. Cossi, B. Mennucci, C. S. Pomelli, J. Tomasi, *Adv. Quant. Chem.* 1998, **32**, 227–261; b) Tomasi, J.; Mennucci, B.; Cammi, R. *Chem. Rev.* 2005, **105**, 2999–3094.
- [2] M. J. Frisch, et.al. 2. Gaussian 09, Revision **D.01**, Gaussian, Inc., Wallingford CT, 2009.
- [3] R. L. Martin, *J. Chem. Phys.* 2003, **118**, 4775–4781.
- [4] R. Villamil-Ramos, V. Barba and A. K. Yatsimirsky. Selective fluorometric detection of pyrophosphate by 3-hydroxyflavonediphenyltin(IV) complex in aqueous micellar medium. *Analyst*, 2012, **137**, 5229–5236.
- [5] M. A. El-Gahami, H. M. Albishri. Equilibrium Studies of Dibutyltin(IV)–Zwitterionic Buffer Complexation. *J. Solution. Chem.* 2013, **42**, 2012–2024.